RESEARCH ARTICLE

Microbial Community Response of an Organohalide Respiring Enrichment Culture to Permanganate Oxidation

Nora B. Sutton[1]*, Siavash Atashgahi[2], Edoardo Saccenti[3], Tim Grotenhuis[1], Hauke Smidt[2], Huub H. M. Rijnaarts[1]

1 Environmental Technology, Wageningen University, Wageningen, The Netherlands, 2 Laboratory of Microbiology, Wageningen University, Wageningen, The Netherlands, 3 Laboratory of Systems and Synthetic Biology, Wageningen University, Wageningen, The Netherlands

* Nora.Sutton@wur.nl

Abstract

While *in situ* chemical oxidation is often used to remediate tetrachloroethene (PCE) contaminated locations, very little is known about its influence on microbial composition and organohalide respiration (OHR) activity. Here, we investigate the impact of oxidation with permanganate on OHR rates, the abundance of organohalide respiring bacteria (OHRB) and reductive dehalogenase (*rdh*) genes using quantitative PCR, and microbial community composition through sequencing of 16S rRNA genes. A PCE degrading enrichment was repeatedly treated with low (25 μmol), medium (50 μmol), or high (100 μmol) permanganate doses, or no oxidant treatment (biotic control). Low and medium treatments led to higher OHR rates and enrichment of several OHRB and *rdh* genes, as compared to the biotic control. Improved degradation rates can be attributed to enrichment of (1) OHRB able to also utilize Mn oxides as a terminal electron acceptor and (2) non-dechlorinating community members of the *Clostridiales* and *Deltaproteobacteria* possibly supporting OHRB by providing essential co-factors. In contrast, high permanganate treatment disrupted dechlorination beyond *cis*-dichloroethene and caused at least a 2–4 orders of magnitude reduction in the abundance of all measured OHRB and *rdh* genes, as compared to the biotic control. High permanganate treatments resulted in a notably divergent microbial community, with increased abundances of organisms affiliated with *Campylobacterales* and *Oceanospirillales* capable of dissimilatory Mn reduction, and decreased abundance of presumed supporters of OHRB. Although OTUs classified within the OHR-supportive order *Clostridiales* and OHRB increased in abundance over the course of 213 days following the final 100 μmol permanganate treatment, only limited regeneration of PCE dechlorination was observed in one of three microcosms, suggesting strong chemical oxidation treatments can irreversibly disrupt OHR. Overall, this detailed investigation into dose-dependent changes of microbial composition and activity due to permanganate treatment provides insight into the mechanisms of OHR stimulation or disruption upon chemical oxidation.

Introduction

Anthropogenic contamination of soil and groundwater with organic chlorinated solvents such as tetrachloroethene (PCE) and trichloroethene (TCE) requires innovative, efficient, and cost-effective remediation technologies. To this end, increasing emphasis is being placed on *in situ* technologies which are less invasive and costly than more traditional *ex situ* treatments. Approaches including *in situ* chemical oxidation (ISCO) and *in situ* bioremediation (ISB) can effectively and efficiently remediate locations without significant disruption of above ground activities [1, 2].

Chemical treatment of chlorinated solvents *in situ* is often performed to rapidly oxidize high concentrations of contaminants [2]. Chemical oxidants such as permanganate, persulfate, hydrogen peroxide, and ozone can efficiently decrease contaminant mass more quickly than, for example, biological treatment. However, once the oxidant has finished reacting, rebound of aqueous contaminant concentrations may occur, either due to dissolution of residual pure product or desorption of solvents sorbed to the soil matrix [3–5]. In such instances, a biopolishing step following ISCO could be advantageous to remove residual contaminants and ensure complete remediation.

Microbial capacity to biodegrade PCE has been exploited in the development of ISB technologies for treatment of chlorinated solvent contaminated locations. Under anaerobic conditions, PCE is degraded by sequential substitution of chlorine atoms for hydrogen atoms to produce, upon complete dechlorination, ethene in an energy conserving process known as organohalide respiration (OHR; [6]). Full scale ISB treatment of PCE contaminated locations often includes subsurface amendment with electron donor and nutrients known as biostimulation; in some cases bioaugmentation with organohalide respiring bacteria (OHRB) able to perform OHR of the target compound is required to ensure complete dechlorination [7].

A restricted but growing number of OHRB have been enriched and isolated in pure culture with the capacity to reductively dechlorinate PCE to TCE, *cis*-dichloroethene (DCE), vinyl chloride (VC) and finally ethene, with *Dehalococcoides mccartyi* being the only organism known to perform full transformation of PCE to ethene [8]. A variety of biomolecular techniques has been developed to specifically monitor OHRB and their reductive dehalogenase (*rdh*) genes. These tools can be used to quantitatively verify biodegradation capacity by monitoring changes in target abundance, thereby assisting in contaminated site management, for example, by indicating whether or not bioaugmentation may be necessary [9, 10].

While axenic cultures of OHRB provide valuable fundamental knowledge about the biochemistry and physiology of these bacteria, OHRB exhibit higher dechlorination rates when present as members of microbial communities. This is in part due to the fastidious nature of key OHRB. In particular, known strains of *D. mccartyi* have been shown to have notable nutritional requirements. Recent metagenomic analysis of enrichment cultures revealed the important role of non-dechlorinators in fulfilling such growth requirements of OHRB [11, 12]. These community members produce fermentation intermediates such acetate and hydrogen, provide essential co-factors (including corrinoids and methionine) and perform oxygen scavenging, while profiting from the removal of toxic chlorinated compounds by OHRB [11, 13, 14]. Building upon this knowledge, a number of studies have yielded insights on microbial community composition and syntrophic interactions, supporting chlorinated solvent degradation in the lab [15–17] and in the field [18, 19].

Whereas ISB has been successfully implemented following ISCO for the remediation of aliphatic and aromatic hydrocarbons [20–23], coupling chemical oxidation with an anaerobic bioremediation step for the treatment of chlorinated solvents is more challenging. In addition to the direct oxidative stress inflicted by the oxidant, increased oxidation-reduction potential

associated with chemical oxidation may be detrimental to strictly anaerobic OHRB or other non-dechlorinating community members. A number of studies have examined the regeneration of OHR capacity following chemical oxidation at batch [24], column [25, 26], and field scales [9, 27]. These investigations revealed threshold oxidant concentrations [24] and the necessity for amendments such as electron donor and bioaugmentation to support biodegradation [25, 26]. In some instances, the abundances of OHRB and *rdh* genes were measured to quantify the impact of chemical oxidation on and subsequent regeneration of OHR capacity [9, 24, 26]. However, these investigations do not provide information on the non-dechlorinating community members that were shown to play indispensable roles in supporting robust and stable dechlorinating consortia [11, 12]. In addition to the interactions described above, the entire microbial community plays a role in attenuation of oxidation-reduction potential following chemical oxidation to ensure regeneration of OHR activity.

Here we investigated the impact of chemical oxidation with permanganate on a PCE degrading consortium using both quantitative PCR (qPCR) and sequencing of 16S rRNA gene fragments. By determining changes in OHRB and *rdh* gene abundance as well as microbial community structure following chemical oxidation, this study improves our insight into the impact of ISCO on microbial communities and their subsequent regeneration following oxidative stress. To our knowledge, the results presented here are a new step towards better understanding and thus application of biopolishing following chemical oxidation.

Materials and Methods

2.1 Microcosm Setup

A total of fourty microcosms were prepared in 125 mL glass serum bottles with Viton stoppers (Rubber b.v., The Netherlands) using a PCE dechlorinating enriched culture, maintained on lactate and PCE at 25°C prior to this study. Prior to inoculation, a final concentration of 10 mM sodium lactate and 2.0 μmol of PCE, both dissolved in anoxic water, were added to the medium [28]. Bottles were inoculated with 5 mL of the enriched culture, thereby reaching a final volume of 50 mL, corresponding to a PCE concentration of 40 μmol/L. Microcosms were incubated at 25°C shaking at 120 rpm prior to treatment with chemical oxidants; chlorinated ethenes were measured in 5 microcosms to ensure OHR activity. Two microcosms were sacrificed for DNA sampling at the start of the experiment (labeled "S") to determine the initial microbial community, as described below.

2.2 Treatment and sampling

Four different conditions were tested with nine replicate microcosms prepared for each treatment: a biotic control which did not receive permanganate and three chemical oxidation treatments with low (25 μmol), medium (50 μmol) and high (100 μmol) permanganate doses. The biotic, low and medium microcosms received PCE additions of 0.86 μmol on days 0, 3, 4, 7, 9, 10, 13, 16, and 17 and permanganate was applied on days 0, 4, 7, 10, 13, and 17 (see Table 1 for details on timing of PCE and permanganate additions and sampling). Sampling for DNA extraction from these microcosms was performed at days 7, 13 and 21 that were considered as the end of treatment cycles 1, 2, and 3, respectively. To ensure sufficient biomass for molecular analyses, each time two microcosms were randomly selected and sacrificed for DNA extraction. Microcosms receiving high permanganate doses showed a larger disruption of OHR activity after the first permanganate addition (Table 1). Hence, permanganate treatments were only performed on days 0, 13, and 33 and additional incubation time was considered to allow regeneration of the microbial community (Table 1). Sampling for the first molecular analyses was performed on day 13. A second DNA sampling was performed on day 21 to temporally

Table 1. Treatment and sampling scheme of microcosms. Biotic control ("B"), low ("L"; 25 µmol) or medium ("M"; 50 µmol) permanganate treatments (above) and high ("H"; 100 µmol) permanganate treatment (below) are given. DNA samples were taken in most cases in duplicate, with microcosm numbers (in bold) corresponding to Table 2. PCE spiking (0.86 µmol) and permanganate (PM) dosing are indicated (x).

	Days	0	1	2	3	4	5	6	7	8	9	10	11	12	13	14	15	16	17	18	19	20	21	22	…	33	…	163	…	246
Biotic, Low, Medium	DNA	**S1+2**							**B, L, M1+2**						**B, L, M 3+4**								**B, L, M5+6**							
	PM (25 or 50 µmol)	x				x						x			x				x											
	PCE (0.86 µmol)	x			x	x					x	x			x			x	x											
High	DNA	**S1+2**													**H1+2**								**H3+4**			**H5+6**		**H7**		**H8+9**
	PM (100 µmol)	x													x											x				
	PCE (0.86 µmol)	x			x										x											x				

doi:10.1371/journal.pone.0134615.t001

coincide with sampling performed in biotic, low and medium treatment microcosms. The third DNA sampling was performed on day 33 followed by the third and final permanganate treatment. Hereafter, these microcosms were monitored over an extended period to track possible regeneration of OHR activity. Only one microcosm (H7) resumed OHR activity, and was sampled on day 163, whereas the two remaining microcosms were sacrificed for DNA isolation on day 246.

Lactate measurements in all microcosms receiving permanganate were used to assess when amendment was required to maintain lactate concentrations around 10 mM. Headspace analysis of PCE, TCE, cis-DCE, VC, and ethene concentrations was always performed one day after addition of PCE and regularly during the first 33 days of the experiment; thereafter, measurements were less frequent.

2.3 Chemical Analyses

Lactate was measured in liquid samples on an HPLC with an organic acids column (Ion 300) and refractive index detector. Samples for Mn^{2+} measurements were collected in 2 mL microcentrifuge tubes, acidified with concentrated HNO_3, and determined by inductively coupled plasma-optical emission spectroscopy. PCE, TCE, cis-DCE, VC and ethene were measured in the headspace. PCE, TCE, and cis-DCE were extracted for 2 minutes with a 100 μm polydimethylsiloxane (PDMS) coated fiber. The compounds were injected at 250˚C on a Fisions 8000 series GC with a CP-Sil8 column (25 m x 0.53 mm x 5.0 μm) using helium as the carrier gas and detected using a Flame Ionization Detector (FID). The program started at 50˚C, ramped at 20˚C/min to 140˚C, and remained at 140˚C for the final 1.5 min. For VC and ethene, 100 μL of headspace was sampled with a glass syringe and directly injected on a HP6890 series GC with a CP PoraBond Q column (25 m x 0.53 mm x 10 μm). The temperature program was isothermal at 60˚C and detection was with a FID at 300˚C. Rates of PCE and TCE conversion were calculated by comparing the total mass of either PCE or TCE measured one day after each PCE spike to the sum of those measured and spiked the previous day (S1 Fig).

2.4 DNA sampling and extraction

Samples for molecular analyses of total DNA were collected by sacrificing two replicate microcosms of each condition. The total volume of each microcosm was vacuum filtered over a separate sterile 0.22 μm membrane filter (Milipore, USA). Each filter was folded and placed in a sterile microcentrifuge tube, snap-frozen in liquid nitrogen, and stored at -20°C until DNA extraction. The volume of filtered liquid was measured using a graduated cylinder to allow calculation of gene copy numbers/mL. DNA extraction was performed using the FastDNA Spin Kit for Soil (MP Biomedicals, USA) according to manufacturer's instructions; the filter was sliced into pieces prior to placement in the bead beater to aid extraction. DNA was eluted with DNase/Pyrogen-Free water, controlled for quantity and quality using a Nanodrop spectrophotometer (Thermo Scientific, Germany), and stored at -20°C.

2.5 Quantitative PCR

Quantitative PCR (qPCR) was performed to measure total bacteria, total archaea, and specific OHRB based on the 16S rRNA gene and rdh genes as described previously [9, 29]. Assayed OHRB were D. mccartyi, Geobacter, Desulfitobacterium, Dehalobacter, Sulfurospirillum, and assayed rdh genes were tceA, bvcA, and vcrA, encoding TCE and VC reductive dehalogenases in D. mccartyi, respectively. Ten-fold dilutions of total DNA extracts were assayed in triplicate using an iQ5 SYBR Green Supermix kit on the iQ5 iCycler (Biorad, The Netherlands). Assayed targets and primer sequences have been described previously [9, 29] and are summarized in S1

Table. Gene copy numbers are expressed as copy/mL culture. To account for natural shifts in abundance due to incubation, results were normalized to the biotic control by dividing the observed abundances in permanganate-treated microcosms at a given time point to that observed in the biotic control.

2.6 Bacterial 16S rRNA gene amplicon pyrosequencing

Bacterial 16S rRNA gene fragments were amplified using barcoded primers covering the V1-V2 region of the bacterial 16S rRNA gene. The forward primer consisted of the 27F-DegS primer (5´- GTTYGATYMTGGCTCAG- 3´) [30] appended with the titanium sequencing adaptor A (5´- CCATCTCATCCCTGCGTGTCTCCGACTCAG- 3´) and an 8 nucleotide sample specific barcode [31] at the 5´ end. An equimolar mix of two reverse primers was used i.e. 338RI (5´- GCWGCCTCCCGTAGGAGT- 3´) and 338RII (5´- GCWGCCACCCGTAGG TGT- 3´) [32] that carried the titanium adaptor B (5´- CCTATCCCCTGTGTGCCTTGGCAG TCTCAG- 3´) at the 5´ end. Sequences of both titanium adaptors were kindly provided by GATC Biotech (Konstanz, Germany). The PCR mix (100 µl final volume) contained 20 µl of 5× HF buffer (Finnzymes, Vantaa, Finland), 2µl PCR Grade Nucleotide Mix (Roche Diagnostic GmbH, Mannheim, Germany), 1µl of Phusion hot start II High-Fidelity DNA polymerase (2U/µl; Finnzymes), 500 nM of the reverse primer mix and the forward primer (Biolegio BV, Nijmegen, The Netherlands), 2 µl (40 ng) template, and 65 µl nuclease free water. PCR was performed using the following conditions: 98°C for 30 s to activate the polymerase, followed by 30 cycles of denaturation at 98°C for 10 s, annealing at 56°C for 20 s, elongation at 72°C for 20 s, and a final extension at 72°C for 10 min. Five µl of the PCR reactions, were analyzed by 1% (w/v) agarose gel electrophoresis, containing 1× SYBR Safe (Invitrogen, Carlsbad, CA, USA) to verify the right length of the amplicons (approximately 450 bp). PCR products were purified using GeneJET PCR purification kit (ThermoScientific, Germany) according to the manufacturer's instructions. The DNA concentration of the purified amplicons was measured using NanoDrop, and amplicons were mixed in equimolar amounts and run again on an agarose gel prior to excision and purification by using a DNA gel extraction kit (Millipore, Billerica, MA, USA). Amplicons obtained from the 24 samples were analysed simultaneously with 30 unrelated samples by pyrosequencing on half a plate using an FLX genome sequencer in combination with titanium chemistry (GATC-Biotech, Konstanz, Germany).

2.7 Analysis and interpretation of the pyrosequencing data

Pyrosequencing data was analysed using the QIIME 1.8.0 pipeline [33]. Sequence reads were initially filtered using default parameters and denoised [34] for removing low quality or ambiguous reads. Chimeric sequences were then removed from pre-processed data from the dataset using UCHIME [35]. From the remaining set of high quality 16S rRNA gene sequences, operational taxonomic units (OTUs) were defined at a 97% identity level. A representative sequence from each OTU was aligned using PyNAST [36]. The taxonomic affiliation of each OTU was determined at an identity threshold of 97% using uclust [35] and SILVA 111 database as a reference [37]. The complete dataset is available at the European Bioinformatics Institute (www. ebi.ac.uk) under accession number PRJEB8632.

2.8 Statistical analysis

In order to interpret the changes in microbial communities to experimental variables, redundancy analysis (RDA) was used as implemented in the CANOCO 5 software package (Biometris, Wageningen, The Netherlands). The experimental variables tested were number of permanganate additions labeled as doses, the cumulative permanganate addition (as µmol),

length of incubation as days, and cumulative PCE addition as number of spikes. A Monte Carlo permutation test based on 499 random permutations was used to determine which of the experimental variables significantly contributed to the observed variance in the composition of microbial communities at the order level. Orders of at least 0.05 relative abundance in any sample were included in the analysis (S2 Table). The community structure was visualized via ordination triplots with scaling focused on intersample differences.

Additionally, a linear mixed model was fitted to order level relative abundances above the 0.05 level. The 29 bottles were considered to be randomly assigned to the different levels of the fixed experimental factor described above. Additionally, the type of treatment (biotic control, low, medium or high permanganate dosage) was also included as fixed factors. The bottles were considered as random term and interactions were not estimated. Calculations were performed using the REML procedure of Genstat 16th SP1 (VSN International, Hemel Hempstead, UK).

Results

3.1 Regeneration of OHR activity following permanganate treatment

The impact of chemical oxidation on OHR activity was investigated by comparing microcosms receiving permanganate treatment with the biotic control without chemical treatment. Permanganate doses are relatively low compared to field application [27], but were similar to those applied in column [26] and batch [24] experiments. The low oxidant concentrations resulted in very little PCE oxidation, as the majority of permanganate was consumed by other reduced constituents. Low chemical oxidation efficiency of PCE was deemed irrelevant, as the goal of this research was to determine the impact of permanganate treatment on the microbial community.

During six doses of permanganate (three cycles of two doses per cycle) over the course of 21 days, OHR was not severely interrupted in microcosms receiving low and medium permanganate treatments of 25 μmol or 50 μmol (Fig 1). Rather, VC production and dechlorination rates were higher in microcosms receiving mild permanganate treatments as compared to the biotic control (Fig 1). For example, on day 8 more than twice as much VC had been produced in microcosms receiving medium permanganate doses, as compared to the biotic control (80% VC versus 37% VC, respectively). In the biotic control, the 80% threshold was not crossed until day 14, a delay of over a week compared to the medium permanganate treatment (Fig 1). Similarly, higher final ethene production was observed in permanganate treated microcosms as compared to the biotic control (31% in medium microcosms versus 20% in the biotic control on day 21). Additionally, PCE and TCE degradation in the first day after spiking was higher in microcosms receiving low or medium permanganate treatments (S1 Fig). In the biotic control microcosms, residual PCE or TCE were often observed the day after a PCE spike (Table 1 and Fig 1), with PCE spiked on days 16 and 17 remaining in the system until the end of incubation on day 21 (Fig 1A). In contrast, in microcosms treated with medium permanganate doses complete conversion of spiked PCE to cis-DCE occurred within 1 day after spiking in nearly all instances (Fig 1C), yielding consistent degradation rates (S1C Fig). These results indicate that chemical oxidation does not disrupt OHR; rather, mild treatments appear to slightly stimulate dechlorination.

In contrast to the more mild permanganate treatments, significant disruption of OHR activity was observed in microcosms receiving high (100 μmol) permanganate doses (Fig 2). Following the first treatment on day 0, cis-DCE production in the high permanganate microcosms (93%; Fig 2) was similar to that of all other treatments (91–95%; Fig 1A–1C). However, following the second PCE spike on day 3, dehalogenation to cis-DCE required a week. Following a
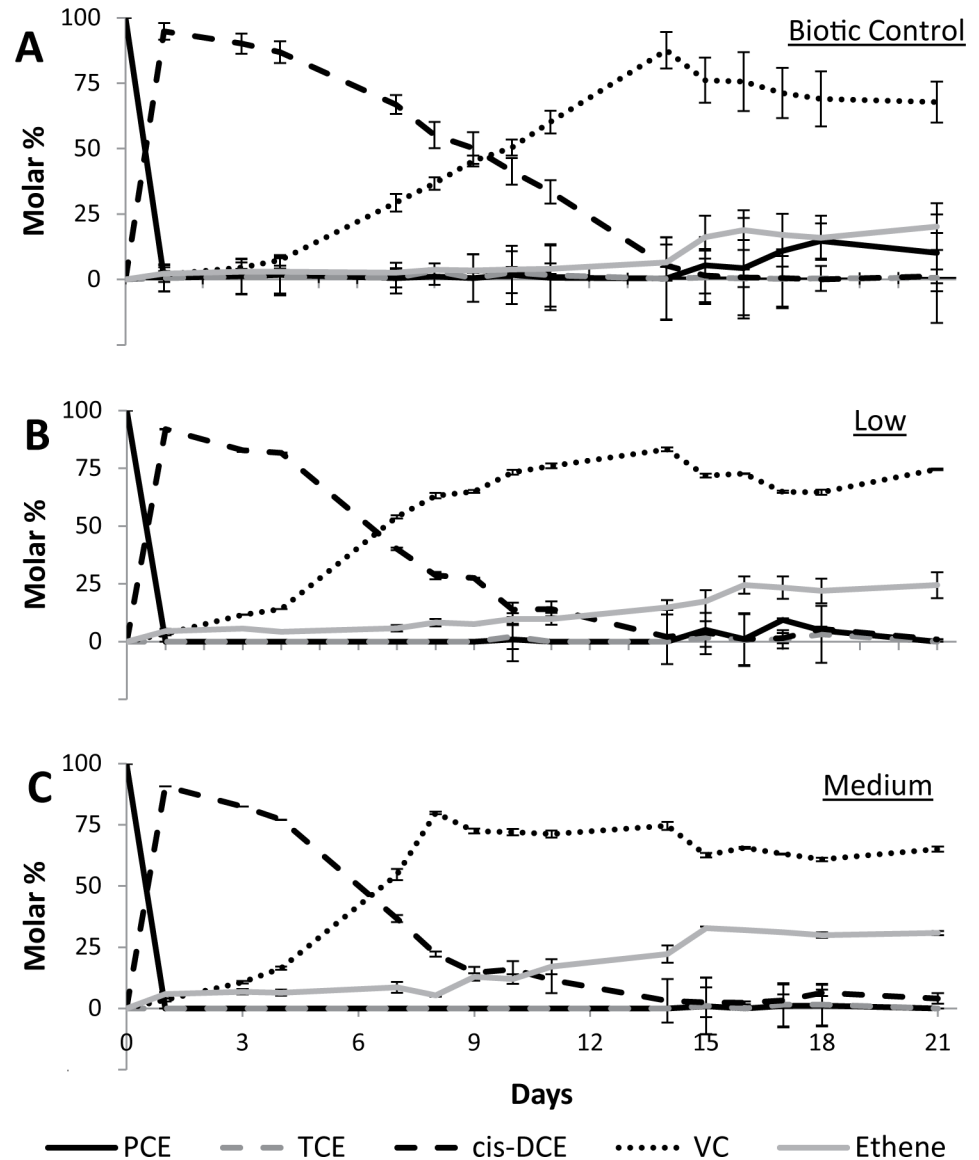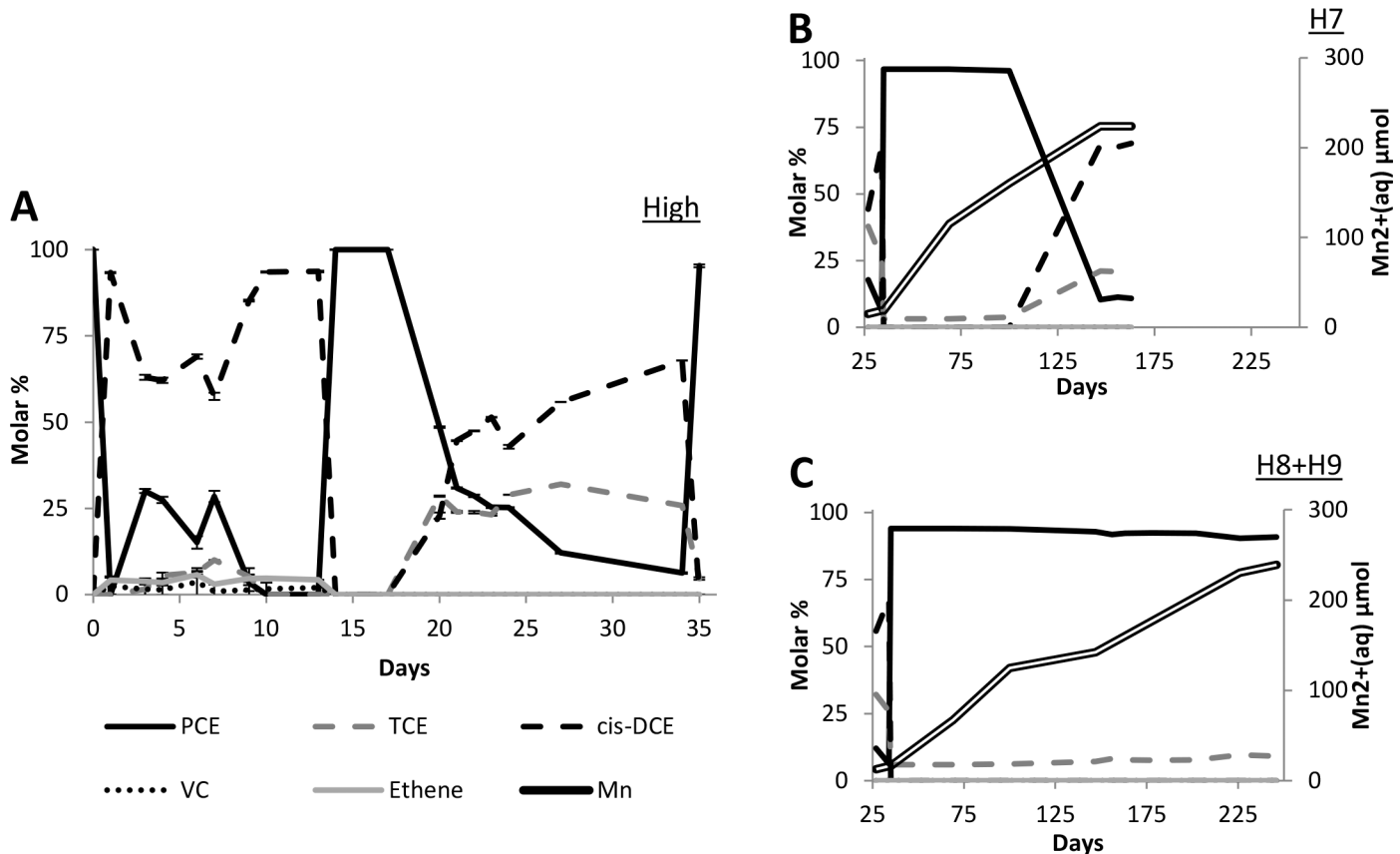
Fig 1. Molar percentage of chlorinated solvent PCE and degradation products TCE, *cis*-DCE, VC, and ethene. Results are given for (A) the biotic control, (B) low (25 µmol) permanganate treatment, and (C) medium (50 µmol) permanganate treatment. As the absolute mass increased over the course of the experiment due to PCE spiking (see Table 1), values are given as the molar percentage of all chlorinated compounds and ethene present at any time point. Headspace analysis of PCE, TCE, *cis*-DCE, VC, and ethene concentrations was always performed one day after each PCE spiking and nearly always in triplicate. the chemical analyses were shuffled between replicate microcosms of each treatment. Hence, the chemical results presented here are a conglomeration of chemical data from in total 9 microcosms.

second permanganate treatment on day 13, dehalogenation was more significantly disrupted (Fig 2). Regeneration of PCE dechlorination coupled to TCE and *cis*-DCE accumulation resumed 4 days after the second permanganate addition on day 13. A third permanganate dose on day 33 severely disrupted OHR. Therefore, OHR activity was monitored over an extended period to determine if regeneration of PCE dechlorination could be observed. While some regeneration was measured on day 147 in H7, no dechlorination was observed in H8 and H9. Throughout the entire experiment, no VC or ethene production was observed at any point in

Fig 2. Molar percentage of chlorinated solvent PCE and degradation products TCE, *cis*-DCE, VC, and ethene and Mn²⁺. Results given for high (100 μmol) permanganate treatment, as described in Fig 1. (A) Days 1–33, during which the most PCE spiking and degradation occurred, are given in more detail. (B and C) Results from extended incubation period including Mn²⁺ concentrations. Results are split for H7 (B) and H8+H9 (C) to show difference in regeneration in degradation between these microcosms.

microcosms receiving high permanganate treatments (Fig 2). Overall these results indicate that stronger chemical oxidant treatments can severely disrupt dechlorination.

Although OHR was disrupted in microcosms receiving high permanganate doses, chemical analyses of dissolved Mn indicated an active microbial community (Fig 2). Mn oxides, the product of permanganate reaction, can be utilized as an electron acceptor in dissimilatory Mn reduction to produce Mn^{2+}. Aqueous Mn^{2+} concentrations steadily increased with prolonged incubation (Fig 2), indicating an actively respiring microbial community. However, as dechlorination of PCE was only observed in H7, Mn reduction was not the only factor limiting the recovery of OHR.

3.2 Influence of permanganate treatment on OHRB and rdh gene abundance

To understand the impact of chemical oxidation on microbial populations associated with OHR, the abundance of a variety of relevant OHRB and *rdh* genes was determined with qPCR. Total bacteria, total archaea, *D. mccartyi*, *Geobacter*, *Desulfitobacterium*, and *Sulfurospirillum* were measured based on their 16S rRNA gene sequence, and primers for specific *rdh* were used to detect *tceA*, *bvcA*, and *vcrA*, encoding TCE and two VC reductive dehalogenases in *D. mccartyi*, respectively (S1 Table and S2 Fig). In biotic controls and microcosms receiving low
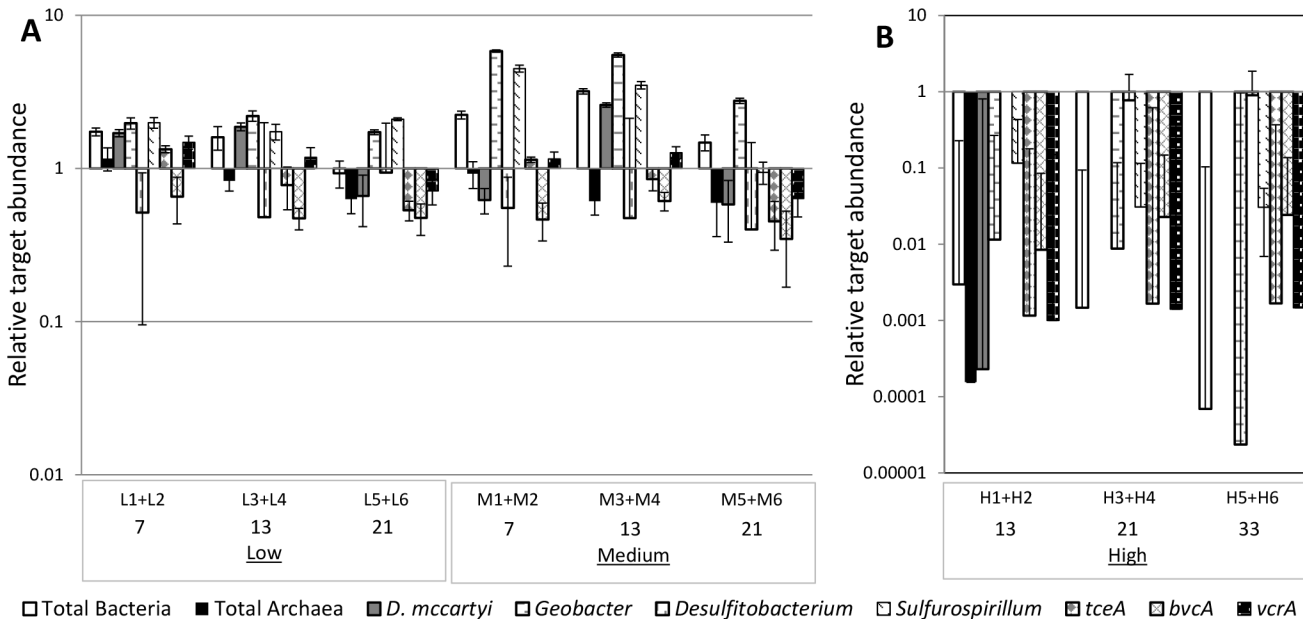
Fig 3. Relative target abundance of OHRB (based on 16S rRNA gene) and *rdh* genes measured by qPCR. Values indicate the enrichment or reduction of a target relative to that measured in the biotic control. Data is averaged between duplicate microcosms for each time point prior to comparison with the biotic control. Error bars are the propagation of standard deviation in triplicate assays, averaging of duplicates, and calculation of relative abundance. (A) Results in low or medium permanganate treated microcosms are compared to results from the biotic control at the same time point. (B) Results from the high permanganate microcosms were compared to the biotic control on day 13 (H1+H2) and day 21 (H3+H4, H5+H6). H7, H8, and H9 are not included, as biotic controls are not available for these time points. Note that different concentration scales are used for Y axes of (A) and (B) panels.

doi:10.1371/journal.pone.0134615.g003

or medium permanganate treatments (25 or 50 µmol), an increase in the absolute abundance of total bacteria, *D. mccartyi*, and *Geobacter* was observed compared to the initial measurement on day 0, indicating their further growth over the course of the experiment (S2 Fig). *Dehalobacter* was not detected in any microcosms, independent of permanganate treatment.

To account for natural shifts in target gene abundance during the course of the experiment, the abundance of each target gene observed in microcosms receiving permanganate was normalized to the corresponding target gene in the biotic controls at each time point (Fig 3). Overall higher total bacteria and *Geobacter* normalized abundances were observed in microcosms receiving low and medium permanganate treatments. In the case of *Geobacter*, a well-described Mn reducer [38], 3–6 times higher abundances were measured on days 7, 13, and 21 in microcosms receiving medium permanganate treatment than in the biotic control (Fig 3A). During the first two weeks, a slight enrichment of *D. mccartyi* and *vcrA* was detected in microcosms receiving low or medium permanganate treatments. However, at the last sampling time point on day 21, the abundances of both targets were lower than those of the biotic control. *Desulfitobacterium*, *bvcA*, and *tceA* were consistently lower in permanganate treated microcosms than in the biotic controls (Fig 3A). In the case of *bvcA* and *tceA*, this result was particularly noteworthy considering the higher PCE degradation rate observed in permanganate treated microcosms (S1 Fig).

In contrast, the abundance of all targets decreased in microcosms receiving high (100 µmol) permanganate doses (S2 Fig), showing the detrimental effect of stronger chemical oxidant treatments on the microbial community. In microcosms H3-H6, neither archaea nor *D. mccartyi* were detected on days 21 and 33, and *Sulfurospirillum* was only detected in one of these four microcosms (H5; S2 Fig). Additionally, high permanganate treatment caused a 2–4 orders of magnitude decrease in the normalized abundance of all detected targets (Fig 3B). With

Table 2. Summary of treatments and timing. Samples were taken at start of experiment ("S"), and during treatment as biotic control ("B"), and receiving low ("L"), medium ("M"), or high ("H") permanganate doses. Treatment times, cumulative permanganate (PM) and number of permanganate doses are used as model inputs for Table 3 and Fig 6 and S3 Fig. Number of sequences and operational taxonomic units (OTUs) obtained for each sample are given.

Sample Code	Treatment	Incubation Time(days)	Cumulative PM(µmol)	Doses PM	Sequences	OTUs
S1	Start	0	0	0	6689	80
S2	(Initial Samples)	0	0	0	8111	103
B1		7	0	0	10585	97
B2		7	0	0	7957	81
B3	Biotic Control	13	0	0	8311	68
B4	(No PM)	13	0	0	10247	60
B5		21	0	0	6791	54
B6		21	0	0	10059	77
L1		7	50	2	9451	67
L2		7	50	2	9194	73
L3	Low	13	100	4	9837	71
L4	(25 µmol PM)	13	100	4	11578	71
L5		21	150	6	10678	67
L6		21	150	6	11513	77
M1		7	100	2	11831	93
M2		7	100	2	10311	81
M3	Medium	13	200	4	12062	97
M4	(50 µmol PM)	13	200	4	10763	94
M5		21	300	6	9147	62
M6		21	300	6	9130	58
H1		13	100	1	9059	70
H2		13	100	1	24380	110
H3		21	200	2	10190	65
H4	High	21	200	2	7875	51
H5	(100 µmol PM)	33	200	2	2788	138
H6		33	200	2	269	26
H7		163	300	3	14507	40
H8		246	300	3	13126	60
H9		246	300	3	16056	37

doi:10.1371/journal.pone.0134615.t002

longer incubation periods, regeneration was observed for many targets to pre-treatment levels (S2 Fig). Notably, *D. mccartyi* was only detected in H7 and *Geobacter* was 3–4 orders of magnitude lower relative to initial samples (S2 Fig). The latter is notable considering this genus's capacity for dissimilatory Mn reduction. Together these results indicate that stronger oxidation treatments severely disrupt the microbial community, which, even upon longer incubation periods, could not be completely restored.

3.3 Microbial community diversity and structure

In order to understand the influence of chemical oxidation on microbial community dynamics, PCR amplified partial 16S rRNA gene fragments were sequenced in samples from the different treatments and time points (Table 1). After filtering and trimming, between 269 and 24380 (average of 10086 ± 4113) high quality sequences were found per sample and clustered into 26–138 operational taxonomic units (OTUs; average 73 ± 23) per sample (Table 2). Although DNA sampling was always performed a number of days after permanganate treatment once
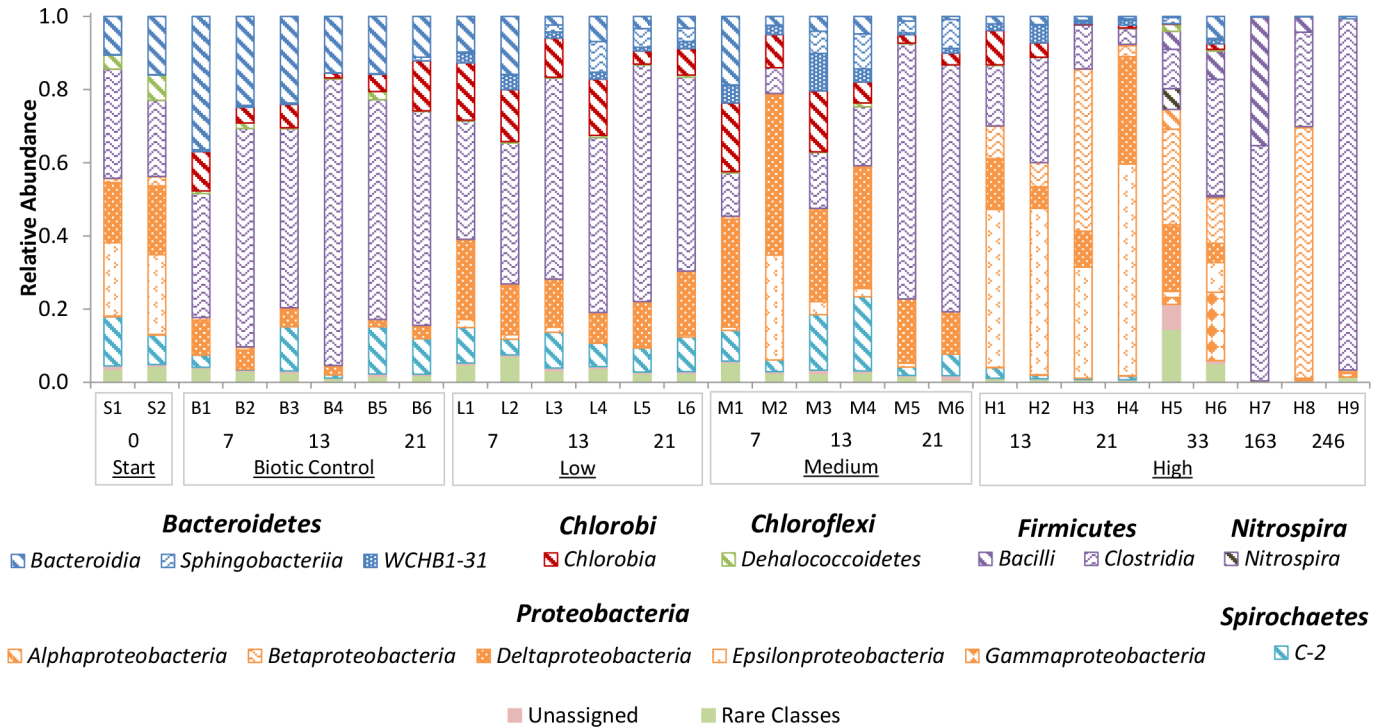
Fig 4. Relative abundance of dominant bacteria phyla and classes. Phyla (given by different colors) and classes (given by pattern) are based on partial 16S rRNA gene sequences obtained by pyrosequencing of barcoded PCR products. Phyla and classes are presented with at least a 0.05 abundance in any sample. Treatments and sample numbers are as given in Table 2. The length of incubation is given in days below the treatment labels.

regeneration of OHR was observed (Table 1), fewer sequences were obtained in samples receiving high permanganate treatment (Table 2). This is most likely due to the direct impact of oxidation on the microbial community. While Mn oxides could theoretically influence DNA extraction efficiency, previous studies on Mn oxide nodules did not indicate this [39, 40]. Regardless, due to the large variation in numbers of sequences obtained for each sample, alpha-diversity could not be properly assessed in this data set.

OTUs were classified into 31 bacterial phyla, with 98.3% of the OTUs belonging to 7 major phyla i.e. *Bacteriodetes*, *Chlorobi*, *Chloroflexi*, *Firmicutes*, *Nitrospirae*, *Proteobacteria*, and *Spirochaetes* (Fig 4). The most abundant OTUs were found to belong to the genus *Acetobacterium* in the class *Clostridia* (*Firmicutes*), the genus *Sulfurospirillum* in the class *Epsilonproteobacteria*, and *Geobacter* of the class *Deltaproteobacteria* (Fig 5). *Clostridia* were prevalent in many samples, with relative abundances up to 96% (H9; Fig 4). Overall, good correspondence was seen between duplicate microcosms, although high permanganate treatments (H3+H4, H5 +H6) and longer incubation times (H8+H9) seemed to cause more divergence between the microbial community in replicate microcosms.

In order to understand the impact of chemical treatment on microbial diversity, statistical models were used to determine the interaction among a number of variables and community structure. Chemical oxidation was assessed in terms of number of doses as well as cumulative permanganate added (Table 2), thereby accounting for the potentially different impact of one large addition versus a number of smaller doses of permanganate. Incubation time was examined, however, for some redundancy analyses H7-H9 were analyzed separately, as the long incubation times skewed the scales and interpretation of the results (Fig 6 and S3 Fig). Finally,
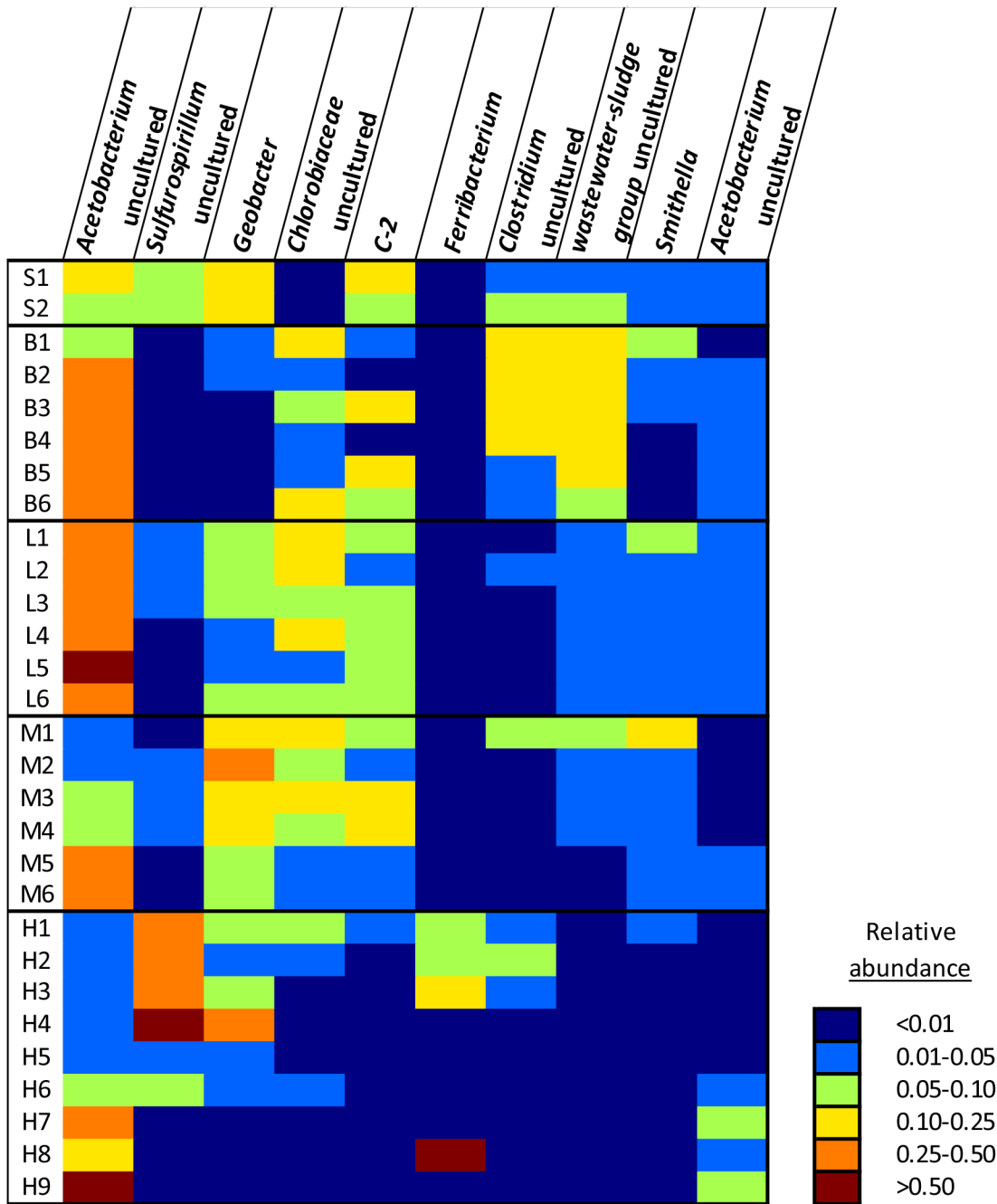
Fig 5. Heatmap of 10 most abundant OTUs in data set. Sample labels as in Table 2 and relative abundances are given as fraction of 1.

PCE dosing was included, however, as PCE spiking was only performed when degradation occurred, this should not be considered a completely independent variable.

Redundancy analysis triplots showed a shift in the community upon incubation (Fig 6). Biotic control microcosms developed away from the starting samples ("S") over time. A strong association could be observed between biotic control microcosms and the order *Bacteroidales* (Fig 6), which is supported by the negative association between cumulative permanganate addition and time and this genus (Table 3). In biotic control microcosms, the order *Bacteroidales*
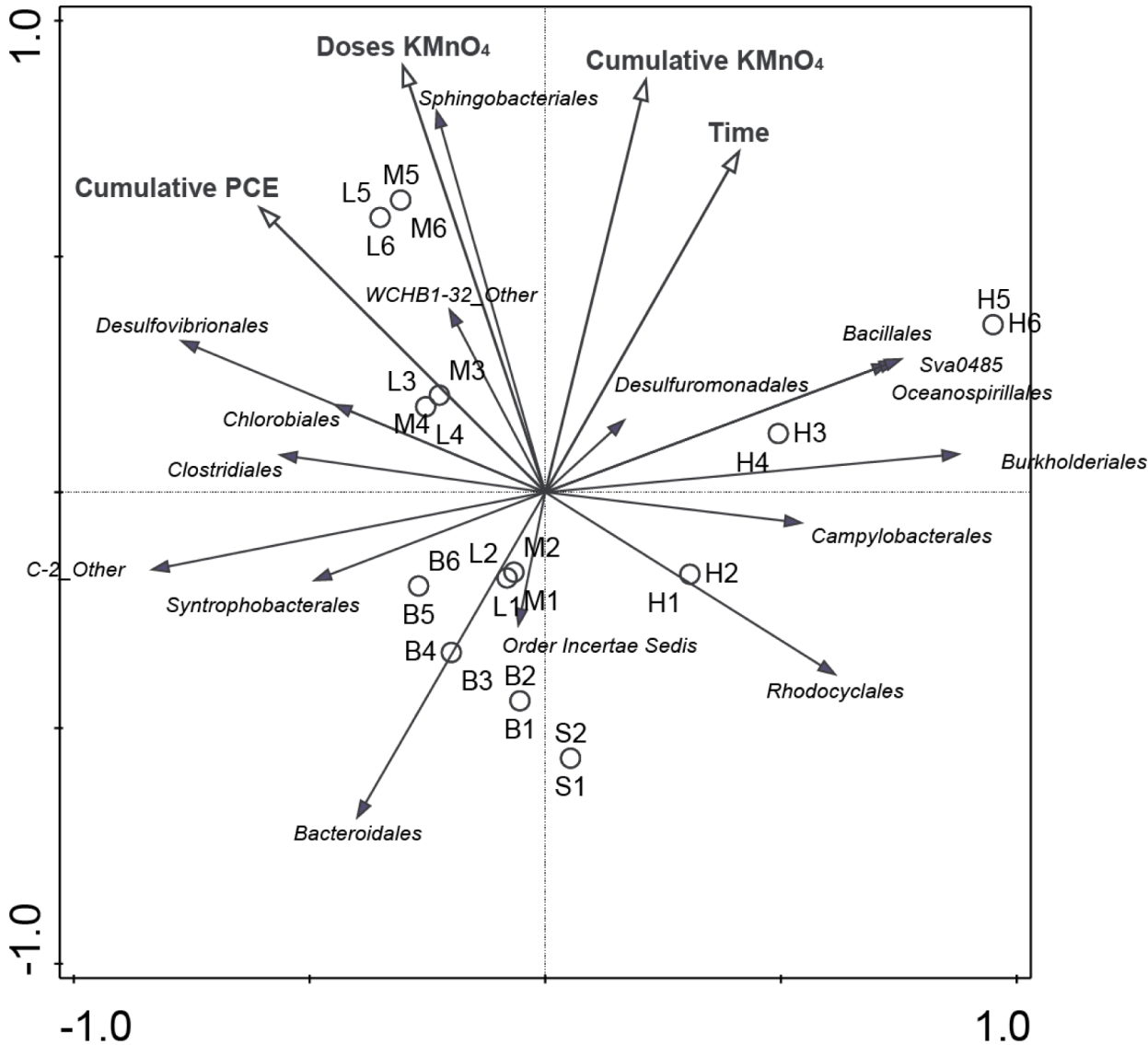
Fig 6. Redundancy Analysis Triplot showing relationship between microbial community composition at order level and treatments. Treatment variables are given as open arrows and are described in Table 2. Closed arrows represent orders. Orders were included with a relative abundance of at least 0.05 in any sample. Arrow length gives the variance that can be explained by a particular treatment parameter. Perpendicular distance reflects association, with smaller distances indicating a larger association. H7, H8 and H9 are left out of this plot because the long incubation times skew the scales, thus compressing the rest of the plot. A Triplot with all samples in this study is given in S3 Fig.

doi:10.1371/journal.pone.0134615.g006

was dominated by the *wastewater sludge group* of the family *Rikenellaceae*, which was notably absent in permanganate treated microcosms (Fig 5). Finally, while the class *Dehalococcoidetes*, dominated by the genus *Dehalococcoides*, was associated with the biotic control, a negative association with incubation time could be observed (Fig 6, Table 3).

Microcosms receiving low or medium permanganate treatments showed close clustering while deviating from the starting sample and biotic control (Fig 6). The variables time, cumulative permanganate addition, and especially permanganate doses showed a stronger association with these treatments. Particularly correlated with low and medium permanganate samples were *Sphingobacteria*, as shown both in triplot (Fig 6) and modelling (Table 3). This order was dominated by unclassified *WCHB1-69* clone, which has been observed in a number of

Table 3. Association between treatment variables and microbial community composition at order level. Treatment variables are from Table 2. Orders were included with relative abundances above 0.05 in any sample. Significant associations are given in bold (P-value < 0.01).

Class	Order	Cumulative KMnO$_4$	Doses KMnO$_4$	Time	Treatment Type
Bacilli	Bacillales	**<0.001**	**<0.001**	**<0.001**	1.000
Bacteroidia	Bacteroidales	**<0.001**	0.593	0.023	0.376
Betaproteobacteria	Burkholderiales	0.017	0.098	0.633	0.125
Betaproteobacteria	Rhodocyclales	0.637	0.298	0.484	0.664
C-2	(Unclassified)	0.091	**<0.001**	0.470	**<0.001**
Chlorobia	Chlorobiales	**0.004**	0.059	0.249	0.072
Clostridia	Clostridiales	**0.002**	0.355	0.131	0.448
Dehalococcoidetes	Order Incertae Sedis	**0.005**	0.986	**<0.001**	0.718
Deltaproteobacteria	Desulfovibrionales	0.025	0.012	0.783	0.061
Deltaproteobacteria	Desulfuromonadales	0.035	0.285	0.012	0.086
Deltaproteobacteria	Sva0485	0.384	0.576	0.084	1.000
Deltaproteobacteria	Syntrophobacterales	**0.008**	0.032	0.054	0.119
Epsilonproteobacteria	Campylobacterales	**0.002**	**<0.001**	**0.002**	0.055
Gammaproteobacteria	Oceanospirillales	0.523	0.671	0.159	1.000
Sphingobacteriia	Sphingobacteriales	0.033	**<0.001**	0.999	0.348
WCHB1-32	(Unclassified)	0.011	0.016	0.185	**0.005**

doi:10.1371/journal.pone.0134615.t003

dechlorinating enrichment cultures [41, 42]. Another unclassified clone of the phylum *Bacteroidetes*, *WCHB1-32*, previously observed in a debrominating culture [43], was also associated with low and medium permanganate treatments. Finally, the order *Clostridales*, dominated by *Acetobacterium*, plots between biotic control and low and medium permanganate dose microcosms (Fig 6). The prevalence of a number of OTUs classified as *Acetobacterium*, an important fermenter identified in a variety of dechlorinating enrichment cultures [11, 44–46] was observed in all three treatments, however at very different relative abundances (Fig 5).

Analysis of the microbial diversity in the microcosms treated with high permanganate doses indicated divergence from the communities observed in low and medium permanganate treatments (Fig 6). The orders *Bacillales*, *Burkholderiales*, *Campylobacterales* and *Oceanospirillales*, as well as the uncultured *Deltaproteobacteria Sva0485* were especially associated with samples receiving high permanganate doses. *Campylobacterales* were dominated by the genus *Sulfurospirillum*, with an uncultured species being the most abundant OTU in samples H1-H4 (Fig 5). *Sulfurospirillum* is known to perform OHR as well as dissimilatory Mn reduction [38, 47]. In addition to *Sulfurospirillum*, *Geobacter* of the order *Desulfuromonadales*, *Campylobacterales* and *Oceanospirillales* were other Mn reducers found to be associated with high permanganate treatment ([38, 48]; Figs 5 and 6). The OTU categorized as *Acetobacterium*, which was found to be highly abundant in other microcosms was found in very low abundance in H1-H6 following high permanganate doses.

Discussion

Permanganate treatment induced changes in dechlorination rates (Figs 1 and 2 and S1 Fig), OHRB and *rdh* gene abundance (Fig 3 and S2 Fig), and microbial community structure (Figs 4–6), as compared to the biotic control. A similar response to chemical oxidation was observed in microcosms receiving low or medium permanganate doses (25 or 50 µmol) which was in sharp contrast to the trend observed upon application of high (100 µmol) permanganate doses. Overall, results indicate a strong dose-dependency: single application of a high quantity of

permanganate can have a severe detrimental effect on OHR, while repeated lower doses yielding the same cumulative quantity of permanganate can have a slightly stimulatory effect.

Permanganate treatment can be detrimental by causing direct cell damage, as seen in the decrease in community size observed following treatment with a variety of chemical oxidants [22, 26, 49]. Additionally, interruption of OHR due to a temporary increase in the redox potential may also be expected. However, the accumulation of Mn oxides seemed to stimulate OHR, as described below. Analysis of microbial community composition in each of the treatments indicated that a balance between detrimental oxidative stress and stimulation with Mn oxides is necessary in order to ensure regeneration of OHR activity following chemical oxidation. Specifically, results indicated that knowledge on a combination of the dynamics of OHRB, Mn reducing bacteria, and non-dechlorinating OHR-supporting community members are key to understanding and predicting the result of permanganate treatment on OHR.

In microcosms receiving high permanganate doses, significant reduction in OHR rates and interruption of dechlorination beyond *cis*-DCE was observed. The sensitivity of OHRB towards oxidative stress has been published previously [50, 51]. A comprehensive study by Amos et al. showed that oxidative stress (up to 30 days of oxygen exposure) disrupts OHR and irreversibly impedes degradation of VC to ethene [50], similar to the stalling at *cis*-DCE observed in our study.

However, it appears that the mechanism of interruption by permanganate treatment is more detrimental to OHRB than that for oxygen. In the study of Amos et al., qPCR analysis showed a less than one order of magnitude drop in the abundance of the *D. mccartyi* 16S rRNA gene and the *rdh* genes *tceA* and *vcrA* upon oxygen exposure, yielding the conclusion that these biomarkers were indicative of presence but were not predictive of cell viability. In contrast, in our high permanganate treatments, a 2 order of magnitude reduction in overall community size and the absence of a number of OHRB 16S rRNA targets was measured (Fig 3 and S2 Fig). These results suggest that permanganate concentrations were high enough to inflict direct cell damage, rather than merely inhibiting OHR by oxidative stress. While the overall community size did regenerate during prolonged incubation (S2C Fig, H7-9), the absence of *D. mccartyi* as the only known microbes capable of complete PCE dechlorination is particularly challenging. It has been shown that at low abundances, *D. mccartyi* can be outcompeted for electron donor and growth substrates [16], implying that permanganate-induced reduction in abundance may not be reversed. These results indicate that increasing the oxidant dose beyond a certain threshold quantity for *D. mccartyi* may irreversibly knockout this organism from OHR consortia, which may lead to the accumulation of more toxic dechlorination intermediates such as *cis*-DCE and VC.

On the other hand, low and medium permanganate treatments were neither detrimental to OHRB and *rdh* abundance nor did these mild treatments interrupt OHR (Fig 3 and S1 Fig). Rather, higher dechlorination rates (Fig 1) and relative abundance of biomarkers (Fig 2) were observed as compared to the biotic control. The observed increase in PCE dechlorination relative to the biotic control can to some extent be explained by the enrichment of a number of target guilds able to utilize permanganate-deposited Mn oxides, in addition to chlorinated ethenes, as terminal electron acceptors. The enrichment of Mn reducing OHRB such as *Geobacter* and *Sulfurospirillum* in low and medium permanganate treatments, as compared to the biotic control (Fig 3), may be attributed to their diverse metabolic capacity [47, 52] and, in the case of *Sulfurospirillum*, apparent resilience to oxidative stress [53]. In addition to the energetic advantage afforded by dissimilatory Mn reduction [54, 55], these genera also have the competitive advantage of being able to switch to chlorinated ethenes as an electron acceptor once Mn oxides have been consumed.

In addition to supporting the higher dechlorination rates observed in low and medium permanganate treatments, Mn reducers contributed to the attenuation of Mn oxides following

chemical oxidation. Members of the orders *Campylobacterales*, *Oceanospirillales*, and *Rhodocyclales*, found in especially high permanganate treatment microcosms (Fig 6), may also have played a role in reduction of Mn oxides. Stable isotope probing of enrichments from three different Mn oxide rich sediments in Sweden, Norway, and Korea identified *Arcobacter* of the order *Campylobacterales* and an unclassified clone in the order *Oceanospirillales* as likely Mn-reducers [48]. Additionally, an OTU classified as the Fe(III) reducer *Ferribacterium* of the order *Rhodocyclales* was particularly prevalent in a number of high permanganate treatment microcosms (Fig 5; [56]). While Mn reduction has not been specifically demonstrated by this genus, the overlapping metabolic capabilities of dissimilatory metal reduction suggest that this OTU may be involved in Mn reduction. It is noteworthy that different Mn reducers were enriched in the high permanganate treated microcosms, where *Geobacter* was not enriched, as compared to the low and medium permanganate treatments. The lower abundances of *Geobacter* in high dose microcosms indicate that this genera may have been particularly susceptible to the detrimental impact of oxidative stress, in line with research showing that this genera lacks homologs of a variety of oxidative stress detoxification enzymes [57].

A number of non-dechlorinating community members identified in permanganate treated microcosms potentially supported OHR through a variety of syntrophic interactions, while profiting from dechlorination of toxic chlorinated compounds. Previous metagenomic analysis of three dechlorinating enrichment cultures identified a number of organisms potentially supportive of *D. mccartyi* with specific metabolic pathways, including corrinoid synthesis, methionine synthesis, oxygen scavenging, and electron donor metabolism [11, 12]. That work identified the role of fermenters associated with *Firmicutes* within the order *Clostridiales*, specifically members of the genus *Acetobacterium* and the family *Clostridiaceae*, as key producers of vitamins and co-factors. In our study, members of the order *Clostridiales* appeared to be correlated with low and medium permanganate treatments and strongly negatively associated with high permanganate treatments (Fig 6). Additionally, an OTU classified as *Acetobacterium* was notably absent in microcosms treated with high permanganate doses just after treatment (H1-H6; Fig 5). While the class *Clostridia* as well as the specific OTU showing similarity to *Acetobacterium* did regenerate upon longer incubation periods (H7-H9; Figs 4 and 6), the low relative abundance of *Dehalococcoides* and perhaps other OHRB precluded regeneration of dechlorination, as suggested previously [16]. Together, these results appear to indicate that strong permanganate treatments are not only detrimental towards OHRB, but also to non-dechlorinating community members essential to the activity of OHRB within consortia.

Thus, analysis of the microbial community diversity in PCE biodegrading microcosms treated with permanganate at different doses gave an indication of mechanisms by which permanganate treatment can either stimulate or interrupt OHR. In low and medium permanganate treatments, specific Mn-reducing, dechlorinating OHRB such as *Geobacter* and *Sulfurospirillum* were enriched that are flexible in using a wider range of electron acceptors. Additionally, stimulated non-dechlorinating supportive guilds such as fermenters within *Clostridiales* and sulfate reducing *Deltaproteobacteria* (Fig 4) could further provide *Dehalococcoides* with essential co-factors, resulting in higher dechlorination rates than in the biotic control, as suggested in other studies [11]. In contrast, high permanganate treatments were strong enough to cause direct cell damage to OHRB as well as equally important non-dechlorinating community members. These results indicate that stronger oxidation treatments may irreversibly knockout *D. mccartyi* from OHR consortia, due to its own strict metabolism and decrease in the abundance of OHR-supporting guilds. In practical applications, the absence of *D. mccartyi* may lead to the accumulation of more toxic dechlorination intermediates such as *cis*-DCE and VC, which pose a higher risk at contaminated locations.

Overall, the results presented here indicate that mild permanganate treatments can have a stimulatory effect on PCE dechlorination, while stronger oxidant loads can completely and irreversibly disrupt OHR. Additionally, our results are the first to report that a number of OHRB appear to be enriched by permanganate treatment and may transiently utilize Mn oxides as an alternative electron acceptor. Enrichment upon permanganate treatment was also indicated for key supportive organisms such as genera within the class *Clostridiales* and *Delta-proteobacteria*, whose consistent abundance throughout permanganate treatment may be indicative of whether or not chemical oxidation will have a stimulatory or detrimental impact on OHR. These important results shed new light on the relationship between OHRB and Mn reducing bacteria in the environment, knowledge which can be exploited in applied field situations to be able to better predict the resiliency of OHR towards permanganate treatment, develop new biomolecular tools targeting organisms key to OHR following chemical oxidation, and eventually design effective and efficient chemical and biological remediation scenarios for full scale field application.

Supporting Information

S1 Fig. PCE and TCE degradation rates. Rates given for PCE (black) and TCE (grey) in the first day after spiking in biotic control (A), low (25 µmol) permanganate (B), and medium (50 µmol) permanganate treatment (C) microcosms. The x-axis indicates the period for which degradation was measured (for example, spiking on day 9 and measurement on day 10). Rates of 0.86 µmol/day indicate full degradation of the 0.86 µmol PCE spike within one day. (PDF)

S2 Fig. OHRB and *rdh* gene abundance for individual microcosms. Individual microcosm numbers are given in Table 2. Error bars are standard deviation of triplicate assays. (PDF)

S3 Fig. Redundancy Analysis Triplot showing relationship between microbial community composition at order level and treatments. Treatment variables are given as open arrows and are described in Table 2. Closed arrows represent orders. Orders were included with a relative abundance of at least 0.05 in any sample. Arrow length gives the variance that can be explained by a particular treatment parameter. Perpendicular distance reflects association, with smaller distances indicating a larger association. (PDF)

S1 Table. Overview of primers used for qPCR assays. (PDF)

S2 Table. Relative abundances of bacterial orders. Orders with relative abundances of more than 0.05 in any sample were included in analyses in Table 3 and Fig 6. (PDF)

Acknowledgments

Author Contributions

Conceived and designed the experiments: NBS SA TG HS HHMR. Performed the experiments: NBS SA ES. Analyzed the data: NBS SA ES TG HS HHMR. Contributed reagents/materials/analysis tools: ES HS HHMR. Wrote the paper: NBS SA ES TG HS HHMR.

References

1. Keijzer T, Pijls C, Marnette E, Sumann M, Volkering F, van Zutphen M. In situ soil and groundwater remediation: theory and practice. Deventer: Tauw bv; 2006. 212 p.

2. Siegrist RL, Crimi M, Brown RA. In situ chemical oxidation: technology description and status. In: Siegrist RL, Crimi M, Simpkin TJ, editors. In situ chemical oxidation for groundwater remediaiton. SERDP and ESTCP Remediation Technology Monograph Series. 1 ed. New York: Springer; 2011. p. 1–32.

3. Mundle K, Reynolds DA, West MR, Kueper BH. Concentration rebound following in situ chemical oxidation in fractured clay. Ground Water. 2007; 45(6):692–702. doi: 10.1111/j.1745-6584.2007.00359.x PMID: WOS:000250498200010.

4. Munakata-Marr J, Sorenson K Jr, Petri B, Cummings JB. Principles of combining ISCO with other in situ remedial approaches. In: Siegrist RL, Crimi M, Simpkin TJ, editors. In situ chemical oxidation for groundwater remediaiton. SERDP and ESTCP Remediation Technology Monograph Series. 1 ed. New York: Springer; 2011. p. 285–317.

5. Kulik N, Goi A, Trapido M, Tuhkanen T. Degradation of polycyclic aromatic hydrocarbons by combined chemical pre-oxidation and bioremediation in creosote contaminated soil. Journal of Environmental Management. 2006; 78(4):382–91. doi: 10.1016/j.jenvman.2005.05.005 PMID: ISI:000235734200007.

6. Smidt H, de Vos WM. Anaerobic microbial dehalogenation. Annu Rev Microbiol. 2004; 58:43–73. doi: 10.1146/annurev.micro.58.030603.123600 PMID: WOS:000225318500003.

7. Major DW, McMaster ML, Cox EE, Edwards EA, Dworatzek SM, Hendrickson ER, et al. Field demonstration of successful bioaugmentation to achieve dechlorination of tetrachloroethene to ethene. Environmental Science & Technology. 2002; 36(23):5106–16. doi: 10.1021/es0255711 PMID: WOS:000179685000028.

8. Loffler FE, Yan J, Ritalahti KM, Adrian L, Edwards EA, Konstantinidis KT, et al. Dehalococcoides mccartyi gen. nov., sp nov., obligately organohalide-respiring anaerobic bacteria relevant to halogen cycling and bioremediation, belong to a novel bacterial class, Dehalococcoidia classis nov., order Dehalococcoidales ord. nov and family Dehalococcoidaceae fam. nov., within the phylum Chloroflexi. International Journal of Systematic and Evolutionary Microbiology. 2013; 63:625–35. doi: 10.1099/ijs.0.034926–0 PMID: WOS:000317170400037.

9. Sutton NB, Atashgahi S, van der Wal J, Wijn G, Grotenhuis T, Smidt H, et al. Microbial dynamics during and after in situ chemical oxidation of chlorinated solvents. Groundwater. 2015; 53(2):261–70. doi: 10.1111/gwat.12209

10. Lee PKH, Macbeth TW, Sorenson KS, Deeb RA, Alvarez-Cohen L. Quantifying genes and transcripts to assess the in situ physiology of "Dehalococcoides" spp. in a trichloroethene-contaminated groundwater site. Applied and Environmental Microbiology. 2008; 74(9):2728–39. doi: 10.1128/aem.02199-07 PMID: ISI:000255567900020.

11. Hug LA, Beiko RG, Rowe AR, Richardson RE, Edwards EA. Comparative metagenomics of three Dehalococcoides-containing enrichment cultures: the role of the non-dechlorinating community. Bmc Genomics. 2012; 13:327–46. doi: 32710.1186/1471-2164-13-327 PMID: WOS:000309925400001.

12. Brisson VL, West KA, Lee PKH, Tringe SG, Brodie EL, Alvarez-Cohen L. Metagenomic analysis of a stable trichloroethene-degrading microbial community. Isme J. 2012; 6(9):1702–14. doi: 10.1038/ismej.2012.15 PMID: WOS:000308141900008.

13. Yan J, Ritalahti KM, Wagner DD, Loffler FE. Unexpected Specificity of Interspecies Cobamide Transfer from Geobacter spp. to Organohalide-Respiring Dehalococcoides mccartyi Strains. Applied and Environmental Microbiology. 2012; 78(18):6630–6. doi: 10.1128/aem.01535-12 PMID: WOS:000308336400030.

14. Men Y, Feil H, VerBerkmoes NC, Shah MB, Johnson DR, Lee PKH, et al. Sustainable syntrophic growth of Dehalococcoides ethenogenes strain 195 with Desulfovibrio vulgaris Hildenborough and Methanobacterium congolense: global transcriptomic and proteomic analyses. Isme J. 2012; 6(2):410–21. doi: 10.1038/ismej.2011.111 PMID: WOS:000300984200017.

15. David MM, Cecillon S, Warne BM, Prestat E, Jansson JK, Vogel TM. Microbial ecology of chlorinated solvent biodegradation. Environmental Microbiology. 2014:n/a-n/a. doi: 10.1111/1462-2920.12413

16. Delgado AG, Kang DW, Nelson KG, Fajardo-Williams D, Miceli JF, Done HY, et al. Selective Enrichment Yields Robust Ethene-Producing Dechlorinating Cultures from Microcosms Stalled at cis-Dichloroethene. Plos One. 2014; 9(6):10. doi: 10.1371/journal.pone.0100654 PMID: WOS:000338276300103.

17. Men YJ, Lee PKH, Harding KC, Alvarez-Cohen L. Characterization of four TCE-dechlorinating microbial enrichments grown with different cobalamin stress and methanogenic conditions. Applied Microbiology and Biotechnology. 2013; 97(14):6439–50. doi: 10.1007/s00253-013-4896-8 PMID: WOS:000321121800029.

18. Lee J, Lee TK, Loffler FE, Park J. Characterization of microbial community structure and population dynamics of tetrachloroethene-dechlorinating tidal mudflat communities. Biodegradation. 2011; 22 (4):687–98. doi: 10.1007/s10532-010-9429-x PMID: WOS:000291168600002.

19. Kotik M, Davidova A, Voriskova J, Baldrian P. Bacterial communities in tetrachloroethene-polluted groundwaters: A case study. Sci Total Environ. 2013; 454:517–27. doi: 10.1016/j.scitotenv.2013.02. 082 PMID: WOS:000319180000055.

20. Valderrama C, Alessandri R, Aunola T, Cortina JL, Gamisans X, Tuhkanen T. Oxidation by Fenton's reagent combined with biological treatment applied to a creosote-comtaminated soil. J Hazard Mater. 2009; 166(2–3):594–602. doi: 10.1016/j.jhazmat.2008.11.108 PMID: ISI:000266947000002.

21. Xie GB, Barcelona MJ. Sequential chemical oxidation and aerobic biodegradation of equivalent carbon number-based hydrocarbon fractions in jet fuel. Environmental Science & Technology. 2003; 37 (20):4751–60. doi: 10.1021/es026260t PMID: ISI:000186133000032.

22. Sutton NB, Langenhoff AAM, Hidalgo Lasso D, Van der Zaan B, Van Gaans P, Maphosa F, et al. Recovery of microbial diversity and activity during bioremediation following chemical oxidation of diesel contaminated soils. Applied Microbiology and Biotechnology. 2014; 98(6):2751–64. doi: 10.1007/ s00253-013-5256-4 PMID: 24092007

23. Sutton NB, Kalisz M, Krupanek J, Marek J, Grotenhuis T, Smidt H, et al. Geochemical and microbiological characteristics during in situ chemical oxidation and in situ bioremediation at a diesel contaminated site. Environmental Science & Technology. 2014; 48(4):2352–60.

24. Dogan-Subasi E, Bastiaens L, Boon N, Dejonghe W. Microbial dechlorination activity during and after chemical oxidant treatment. J Hazard Mater. 2013; 262:598–605. doi: 10.1016/j.jhazmat.2013.09.003 PMID: WOS:000329595500071.

25. Hrapovic L, Sleep BE, Major DJ, Hood ED. Laboratory study of treatment of trichloroethene by chemical oxidation followed by bioremediation. Environmental Science & Technology. 2005; 39(8):2888–97. doi: 10.1021/es049017y PMID: ISI:000228428900067.

26. Sahl JW, Munakata-Marr J, Crimi ML, Siegrist RL. Coupling permanganate oxidation with microbial dechlorination. Water Environment Research. 2007; 79(1):5–12. doi: 10.2175/106143006x136720 PMID: ISI:000243569200002.

27. Sercu B, Jones ADG, Wu CH, Escobar MH, Serlin CL, Knapp TA, et al. The Influence of In Situ Chemical Oxidation on Microbial Community Composition in Groundwater Contaminated with Chlorinated Solvents. Microb Ecol. 2013; 65(1):39–49. doi: 10.1007/s00248-012-0092-0 PMID: WOS:000313369900005.

28. Holliger C, Schraa G, Stams AJM, Zehnder AJB. A highly purified enrichment culture couples the reductive dechlorination of tetrachloroethene to growth. Applied and Environmental Microbiology. 1993; 59(9):2991–7. PMID: WOS:A1993LW04000035.

29. Yu Y, Lee C, Kim J, Hwang S. Group-specific primer and probe sets to detect methanogenic communities using quantitative real-time polymerase chain reaction. Biotechnol Bioeng. 2005; 89(6):670–9. doi: 10.1002/bit.20347 PMID: WOS:000227247700006.

30. van den Bogert B, de Vos WM, Zoetendal EG, Kleerebezem M. Microarray Analysis and Barcoded Pyrosequencing Provide Consistent Microbial Profiles Depending on the Source of Human Intestinal Samples. Applied and Environmental Microbiology. 2011; 77(6):2071–80. doi: 10.1128/aem.02477-10 PMID: WOS:000288203500017.

31. Hamady M, Walker JJ, Harris JK, Gold NJ, Knight R. Error-correcting barcoded primers for pyrosequencing hundreds of samples in multiplex. Nat Methods. 2008; 5(3):235–7. doi: 10.1038/nmeth.1184 PMID: WOS:000253777900015.

32. Daims H, Bruhl A, Amann R, Schleifer KH, Wagner M. The domain-specific probe EUB338 is insufficient for the detection of all Bacteria: Development and evaluation of a more comprehensive probe set. Syst Appl Microbiol. 1999; 22(3):434–44. PMID: WOS:000083229200015.

33. Caporaso JG, Kuczynski J, Stombaugh J, Bittinger K, Bushman FD, Costello EK, et al. QIIME allows analysis of high-throughput community sequencing data. Nat Methods. 2010; 7(5):335–6. doi: 10.1038/ nmeth.f.303 PMID: WOS:000277175100003.

34. Bragg L, Stone G, Imelfort M, Hugenholtz P, Tyson GW. Fast, accurate error-correction of amplicon pyrosequences using Acacia. Nat Methods. 2012; 9(5):425–6. doi: 10.1038/nmeth.1990 PMID: WOS:000303544800004.

35. Edgar RC. Search and clustering orders of magnitude faster than BLAST. Bioinformatics. 2010; 26 (19):2460–1. doi: 10.1093/bioinformatics/btq461 PMID: WOS:000282170000016.

36. DeSantis TZ, Hugenholtz P, Keller K, Brodie EL, Larsen N, Piceno YM, et al. NAST: a multiple sequence alignment server for comparative analysis of 16S rRNA genes. Nucleic Acids Res. 2006; 34: W394–W9. doi: 10.1093/nar/gkl244 PMID: WOS:000245650200080.

37. Pruesse E, Quast C, Knittel K, Fuchs BM, Ludwig WG, Peplies J, et al. SILVA: a comprehensive online resource for quality checked and aligned ribosomal RNA sequence data compatible with ARB. Nucleic Acids Res. 2007; 35(21):7188–96. doi: 10.1093/nar/gkm864 PMID: WOS:000251868800024.

38. Lovley DR, Holmes DE, Nevin KP. Dissimilatory Fe(III) and Mn(IV) reduction. In: Poole RK, editor. Advances in Microbial Physiology, Vol 49. Advances in Microbial Physiology. 49. London: Academic Press Ltd-Elsevier Science Ltd; 2004. p. 219–86. PMID: 15518832

39. He JZ, Zhang LM, Jin SS, Zhu YG, Liu F. Bacterial communities inside and surrounding soil iron-manganese nodules. Geomicrobiol J. 2008; 25(1):14–24. doi: 10.1080/01490450701829014 PMID: WOS:000257225800002.

40. Stein LY, La Duc MT, Grundl TJ, Nealson KH. Bacterial and archaeal populations associated with freshwater ferromanganous micronodules and sediments. Environmental Microbiology. 2001; 3(1):10–8. doi: 10.1046/j.1462-2920.2001.00154.x PMID: WOS:000167056100002.

41. Xu MY, Chen XJ, Qiu MD, Zeng XW, Xu J, Deng DY, et al. Bar-Coded Pyrosequencing Reveals the Responses of PBDE-Degrading Microbial Communities to Electron Donor Amendments. Plos One. 2012; 7(1). doi: 10.1371/journal.pone.0030439 PMID: WOS:000301640600031.

42. Bunge M, Wagner A, Fischer M, Andreesen JR, Lechner U. Enrichment of a dioxin-dehalogenating Dehalococcoides species in two-liquid phase cultures. Environmental Microbiology. 2008; 10 (10):2670–83. doi: 10.1111/j.1462-2920.2008.01688.x PMID: WOS:000259147900018.

43. Knight VK, Kerkhof LJ, Haggblom MM. Community analyses of sulfidogenic 2-bromophenol-dehalogenating and phenol-degrading microbial consortia. Fems Microbiology Ecology. 1999; 29(2):137–47. doi: 10.1111/j.1574-6941.1999.tb00605.x PMID: WOS:000081005100003.

44. Fletcher KE, Ritalahti KM, Pennell KD, Takamizawa K, Loffler FE. Resolution of culture Clostridium bifermentans DPH-1 into two populations, a Clostridium sp and tetrachloroethene-dechlorinating Desulfitobacterium hafniense strain JH1. Applied and Environmental Microbiology. 2008; 74(19):6141–3. doi: 10.1128/aem.00994-08 PMID: WOS:000259528700036.

45. Philips J, Hamels F, Smolders E, Springael D. Distribution of a dechlorinating community in relation to the distance from a trichloroethene dense nonaqueous phase liquid in a model aquifer. FEMS Microbiology Ecology. 2012; 81(3):636–47. doi: 10.1111/j.1574-6941.2012.01395.x PMID: WOS:000307168900011.

46. Macbeth TW, Cummings DE, Spring S, Petzke LM, Sorenson KS. Molecular characterization of a dechlorinating community resulting from in situ biostimulation in a trichloroethene-contaminated deep, fractured basalt aquifer and comparison to a derivative laboratory culture. Applied and Environmental Microbiology. 2004; 70(12):7329–41. doi: 10.1128/aem.70.12.7329–7341.2004 PMID: WOS:000225719300048.

47. Luijten M, de Weert J, Smidt H, Boschker HTS, de Vos WM, Schraa G, et al. Description of Sulfurospirillum halorespirans sp nov., an anaerobic, tetrachloroethene-respiring bacterium, and transfer of Dehalospirillum multivorans to the genus Sulfurospirillum as Sulfurospirillum multivorans comb. nov. International Journal of Systematic and Evolutionary Microbiology. 2003; 53:787–93. doi: 10.1099/ijs.0.02417–0 PMID: WOS:000183268200022.

48. Vandieken V, Pester M, Finke N, Hyun JH, Friedrich MW, Loy A, et al. Three manganese oxide-rich marine sediments harbor similar communities of acetate-oxidizing manganese-reducing bacteria. Isme J. 2012; 6(11):2078–90. doi: 10.1038/ismej.2012.41 PMID: WOS:000310056400010.

49. Tsitonaki A, Smets BF, Bjerg PL. Effects of heat-activated persulfate oxidation on soil microorganisms. Water Research. 2008; 42(4–5):1013–22. doi: 10.1016/j.watres.2007.09.018 PMID: ISI:000254111000019.

50. Amos BK, Ritalahti KM, Cruz-Garcia C, Padilla-Crespo E, Loffler FE. Oxygen effect on Dehalococcoides viability and biomarker quantification. Environmental Science & Technology. 2008; 42 (15):5718–26. doi: 10.1021/es703227g PMID: ISI:000258075100054.

51. He JZ, Ritalahti KM, Aiello MR, Loffler FE. Complete detoxification of vinyl chloride by an anaerobic enrichment culture and identification of the reductively dechlorinating population as a Dehalococcoides species. Applied and Environmental Microbiology. 2003; 69(2):996–1003. doi: 10.1128/aem.69.2.996–1003.2003 PMID: WOS:000180927100035.

52. Lovley D. Dissimilatory Fe(III)- and Mn(IV)-reducing prokaryotes. In: Rosenberg E, DeLong EF, Lory S, Stackebrandt E, Thompson F, editors. The Prokaryotes-Prokaryotic Physiology and Biochemistry. 4 ed. Berlin: Springer; 2013. p. 287–308.

53. Goris T, Schubert T, Gadkari J, Wubet T, Tarkka M, Buscot F, et al. Insights into organohalide respiration and the versatile catabolism of Sulfurospirillum multivorans gained from comparative genomics and physiological studies. Environmental Microbiology. 2014; 16(11):3562–80. doi: 10.1111/1462-2920.12589 PMID: WOS:000345631900014.

54. He JZ, Sung Y, Dollhopf ME, Fathepure BZ, Tiedje JM, Loffler FE. Acetate versus hydrogen as direct electron donors to stimulate the microbial reductive dechlorination process at chloroethene-contaminated sites. Environmental Science & Technology. 2002; 36(18):3945–52. doi: 10.1021/es025528d PMID: WOS:000178016600009.

55. Lovley DR, Phillips EJP, Lonergan DJ. Hydrogen and formate oxidation coupled to dissimilatory reduction of iron or manganese by *Alteromonas putrefaciens*. Applied and Environmental Microbiology. 1989; 55(3):700–6. PMID: WOS:A1989T468400027.

56. Cummings DE, Caccavo F, Spring S, Rosenzweig RF. Ferribacterium limneticum, gen. nov., sp. nov., an Fe(III)-reducing microorganism isolated from mining-impacted freshwater lake sediments. Archives of Microbiology. 1999; 171(3):183–8. doi: 10.1007/s002030050697 PMID: WOS:000078980500007.

57. Wagner DD, Hug LA, Hatt JK, Spitzmiller MR, Padilla-Crespo E, Ritalahti KM, et al. Genomic determinants of organohalide-respiration in Geobacter lovleyi, an unusual member of the Geobacteraceae. Bmc Genomics. 2012; 13. doi: 10.1186/1471-2164-13-200 PMID: WOS:000306555100001.